Catalysis Today 176 (2011) 219–224

Contents lists available at ScienceDirect

Catalysis Today

journal homepage: www.elsevier.com/locate/cattod

Catalysed diesel particulate filter: Study of the reactivity of soot arising from biodiesel combustion

Nora Lamharess[a], Claire-Noelle Millet[a], Laurie Starck[b], Eric Jeudy[a], Jacques Lavy[a,*], Patrick Da Costa[c]

[a] IFP Energies nouvelles, Rond-point de l'echangeur de Solaize, BP3, 69360 Solaize, France
[b] IFP Energies nouvelles, 1-4 avenue de Bois-Préau, 92852 Rueil-Malmaison, France
[c] Institut Jean Le Rond d'Alembert, Université Pierre and Marie Curie, 2 place de la gare de Ceinture, 78210 Saint Cyr l'Ecole, France

ARTICLE INFO

Article history:
Received 16 September 2010
Received in revised form 9 December 2010
Accepted 7 January 2011
Available online 8 February 2011

Keywords:
CDPF
Soot reactivity
Biodiesel

ABSTRACT

Biodiesel as a renewable energy allows to partly resolve environmental and economic problems by reducing vehicle greenhouse gases, polluting emissions and dependency on fossil oil energy. It can also reduce emissions of PM, THC, and CO emissions when used in diesel engine. The reactivity of soot arising from this fuel and trapped in a catalysed diesel particle filter (CDPF) was investigated and compared to a ULSD soot (Ultra Low Sulphur Diesel). A different behaviour was expected especially due to the amount of oxygen present in the original fuel (rapeseed methyl ester, RME). Indeed results of reactivity tests showed that B30 soot formed from B30 fuel containing 30% vol. of RME was more reactive than ULSD soot. Besides its greater oxygen content (8%), surface area and structure evolution during oxidation were also found to be reasons for the important reactivity of B30 soot. A specific combustion mode was highlighted by transmission electronic microscopy that facilitates access of oxygen in this soot structure and thus its reactivity.

Tests were also conducted to evaluate the interactions occurring between soot and the other pollutants on the CDPF: CO, HC, NOx. B30 soot appeared to have a greater impact than ULSD soot around light-off temperature, especially concerning the competition with other reductants to access oxidants available in the feed: HC and CO oxidation by oxygen on one hand and NO oxidation by oxygen to form NO_2 and oxidize soot on the other hand.

1. Introduction

As an effort to reduce vehicle greenhouse gases, polluting emissions and dependency on fossil oil energy, governments are increasingly making the use of various types of biofuels mandatory with a view to partly resolve environmental and economic problems.

Biodiesel or methyl ester of fatty acid is the most common type of biofuel in Europe. It is produced from trans-esterification of vegetable oils or animal fats. The main resources for biodiesel production can be obtained from plant species such as soy, rapeseed, jatropha, mahua, and mustard.

The overall lifecycle emissions of carbon dioxide, well-to-wheel, from biodiesel are very variable [1–3], locally dependent and often unreliable, but a saving of between 50% and 80% (and even more in the case of waste-oil biodiesel [1,2]) with respect to petroleum diesel emissions could be accepted as a high confidence range.

Biodiesel fuels have an interesting potential to reduce chemical emissions. However, the effect of biodiesel is specific for each of the different pollutant species and depends on the type of engine, engine operating conditions, ambient conditions, origin and quality of biodiesel, etc.

Regulated pollutants are nitrogen oxides (NOx), particulate matter (PM), total hydrocarbons (THC), and carbon monoxide (CO). Previous studies [4,5] have confirmed that combustion of B100 (neat biodiesel) in diesel engines results in an average increase in NOx exhaust emissions of 12% and decreases in PM, THC, and CO emissions of 48, 77, and 48%, respectively, versus petrodiesel. For B20 soybean oil methyl ester (SME) blends, NOx emissions are increased by 0–4% in comparison to petrodiesel, but PM, THC, and CO emissions are reduced by 10, 20 and 11% respectively [6].

In order to satisfy emission standards which become increasingly stringent, actions on the engine alone are not sufficient. It is thus important to approach the problem on the whole and to account also for the fuel and the exhaust gas after treatment. Several after treatment systems have been developed in recent years for diesel engines such as the particulate filter, NOx trap, and the combination of both.

* Corresponding author.
E-mail address: jacques.lavy@ifpenergiesnouvelles.fr (J. Lavy).

0920-5861/$ – see front matter © 2011 Elsevier B.V. All rights reserved.
doi:10.1016/j.cattod.2011.01.011

The Catalysed Diesel Particulate Filter (CDPF) which is used in our study consists of a porous material positioned in the exhaust line and designed to collect particulate matter with an efficiency of 90%. It has a catalytic coating to burn off the collected particulate matter into carbon dioxide and water at a lower temperature.

Several chemical and physical techniques are described in the literature to characterize soot collected on a DPF. Among others, nitrogen-BET or SAXS surface area measurements combined with TEM (transmission electron microscopy) data highlight the structural evolution of soot during its combustion: Kandas et al. [7] observed that the volatilization of condensables removes the adsorbed compounds, providing access to the porous structure. Oxidation then further opens up porosity leading to complete access to the internal surfaces, before reaction continues at approximately constant density because of shrinkage due to structural ordering during oxidation. Van der Wal et al. [8] found that some primary particles have hollow interior outer shell exhibiting evidence of graphitization, depending on the oxidation history of the sample. Song et al. [9] found that this hollowing is significant during the early oxidation stage of oxidation of a B100 soot (neat soybean-derived biodiesel fuel) which is far more reactive than other diesel soots, including soot from neat Fischer–Tropsch diesel (FT100). This higher reactivity has also been found in other works [10,11] and is attributed to the greater surface oxygen functionality of the B100 soot.

However, to our knowledge, although the characteristics and reactivity of biodiesel soot have been studied by several research groups, there is a lack of information about its impact on the catalysed particulate filter. We found that the presence of soot partly can inhibit NOx storage and CO and HC conversion around 300 °C on a 4-way catalytic converter, as described in Millet et al. [12] In a recent paper, Castoldi et al. [13] also highlighted the negative influence of soot on the NOx storage capacity of such a catalyst.

The purpose of this work is hence to assess the impact of biodiesel soot (arising from a 30% RME diesel fuel) on the behaviour of a CDPF, compared to soot issued from a conventional fuel: filter regeneration and interactions with other catalytic reactions. The soot composition and structure were examined (BET surface area, HRTEM), and the soot loaded CDPF behaviour was examined under realistic conditions by tests conducted on a flow reactor.

2. Experimental

2.1. Fuels

The two following fuels were considered:

- An ultra low sulphur diesel fuel (ULSD) with 4 wt ppm sulphur, no oxygen and 22 wt% total aromatics. This fuel is used as a reference to assess the impact of biofuels on exhaust pollutants (NOx, HC. . .) and soot composition, properties and reactivity.
- A 30% biodiesel blended in ULSD fuel (named 'B30') produced from rapeseed methyl ester (RME). This blend could be considered as a future formulation considering an increasing content of biodiesel in conventional diesel fuel. It can also be noticed that at present, diesel blends with 30% of ester are already being used by some dedicated fleets. Moreover, such an important content of biodiesel will allow to more clearly highlight its effects.

2.2. Soot collection

The commercial catalysed diesel particulate filter (CDPF) that was investigated in this study is a porous monolithic honeycomb structure, 1.44 L in volume and 300 cells/in.^{2} (cpsi) in cell density. Filter channels are alternatively plugged so as to ensure particle filtration. Main components of the support material are 40% Al_2O_3, 36% ZrO_2 and 4.5% CeO_2 (mass composition). Active species for oxidation is Pt (2%). The catalyst was directly loaded with soot on an engine bench, either in its full size or cut into small samples. The latter were 25 mm in diameter and 50 mm in length. Channels were replugged where necessary.

The engine used in this study is a PSA Peugeot-Citroën 2.0 L 4-cylinder automotive diesel engine (DW10B). It has 4 valves per cylinder, a common rail fuel injection, a variable geometry turbocharger, a high pressure exhaust gas recirculation circuit (EGR), including a control valve and a cooler, and an intake throttle. In our study, the engine was used to generate 9 g/h of soot on the following stabilized operating point: engine speed 1500 rpm and BMEP 5 bar.

Two types of loading were conducted:

Full size CDPF loading: the CDPF was mounted in the exhaust line and loaded for 2 h. Soot was then removed from the filter by blowing and collected (Fig. 1(a)).

CDPF sample loading: A revolver cylinder like device was used to load 18 samples at once with about 100 mg of soot per CDPF sample (Fig. 1(b)).

2.3. Soot characterization

Soot was characterized by using a number of macroscopic and microscopic techniques: composition analysis (thermal conductiv-

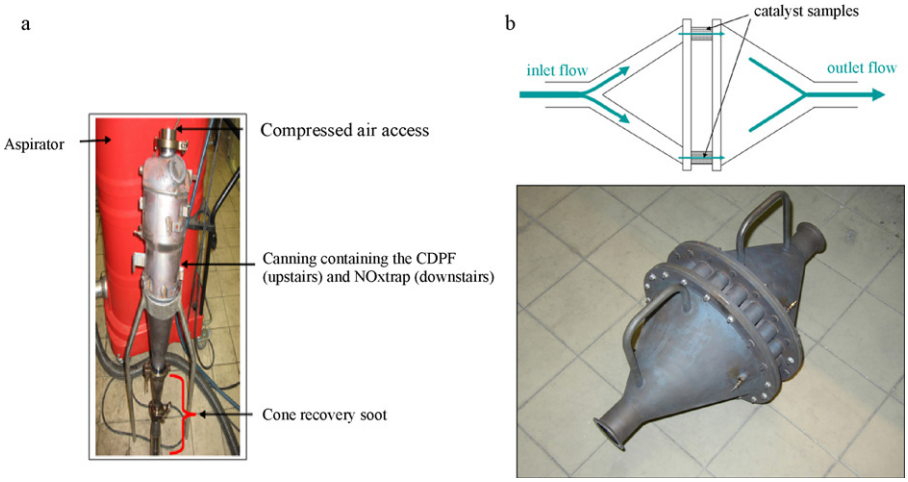

Fig. 1. Devices used to collect soot loaded in a full size CDPF (a) and to load CDPF samples (b) on the engine test bench.

Table 1
Characteristics of ULSD and B30 fuels. ULSD: ultra low sulphur diesel, B30: 30% biodiesel blend in ULSD fuel.

Fuels	ULSD	B30
Oxygen content (wt%)	<0.50	2.25
Aromatics (wt%)	22.0	15.4
Cetane number[a]	51	54
Heating value (MJ/kg)	41.7	40.4

[a] Measured by CFR engine.

Table 2
Characteristics of ULSD and B30 soot. ULSD: ultra low sulphur diesel, B30: 30% biodiesel blend in ULSD fuel.

Soot	ULSD	B30
C (wt%)	91.8	89.3
H (wt%)	0.53	0.58
N (wt%)	<0.05	<0.05
S (wt%)	<0.10	<0.10
O (wt%)	7.20	8.90
BET surface area (m^2/g)	414	448

ity for carbon, hydrogen and nitrogen and by coulometry for oxygen and sulphur), surface area (BET) and structure (transmission electron microscopy or TEM). TEM images were taken with a JEOL JEM 100CX transmission electron microscope, operating at 100 kV mode fringe of lattice, it has an effective resolving power of 3 Å, which allows to view the profile of carbon planes (separated by at least 3.35 Å which is the value for graphite) and gives access to soot structure and microtexture.

The soot reactivity study was carried out on a synthetic gas bench under atmospheric pressure and flow conditions representative of diesel exhaust gases. The sample (soot alone or loaded on a CDPF) was placed in a quartz tube. A thermocouple in front of the sample was used to control the temperature and another one was inserted downstream from the sample. The quartz tube was placed in an electrically heated oven.

Two different types of experiments were performed:

- Isothermal oxidation tests of 10 mg of soot alone with 10% of O_2 and N_2 as balance with a 100 L/h flow rate.
- Light-off tests during a temperature ramp of 10 °C min^{-1} with a CDPF sample loaded with soot. The gas composition was chosen close to a lean diesel environment with a 0.3 equivalence ratio (900 ppmC C_3H_6 + 300 ppm NO + 700 ppm CO + 15% O_2 + 4% CO_2 + 4% H_2O + N_2 balance). Propylene was used to represent unburned hydrocarbons emitted by engine combustion. The flow rate was 750 L/h.

All gases were fed to the reactor via mass flow controllers, while water vapour was injected through a vaporizer in an N_2 flow. Analysed gases were CO, CO_2 (NDIR), O_2 (paramagnetic), HC (FID), NOx, NO and NO_2 (chemiluminescence).

3. Results and discussion

3.1. Fuel characteristics

The fuel characteristics are listed in Table 1.

ULSD oxygen content is very low and increases with the addition of RME, due to the oxygen present in the ester groups. Cetane numbers are quite close considering a measurement uncertainty of ±4.5. This is in agreement with cetane numbers of neat rapeseed esters found in the literature, which range from 48 to 56 [14]. The aromatic content decreases between the ULSD fuel and the B30 fuel due to dilution, since RME is free of aromatic compounds. The RME heating value was found to be 37.6 MJ/kg which is in agreement with literature saying that heating power of neat rapeseed esters ranges between 37 and 39 [14]. The B30 fuel has an intermediate heating value.

3.2. Soot properties

Table 2 presents the composition and surface area of soot arising from ULSD and B30 fuel engine combustion and collected from the CDPF. Major soot components are carbon and oxygen, with a small amount of hydrogen. Nitrogen and sulphur concentrations are below detection levels. Results show that B30 soot has a higher oxygen content than ULSD soot (+24%), which is due to the oxygenated RME. Both soot samples have a rather large surface area and B30 soot surface area is 8% above ULSD soot.

3.3. Effect of biofuel on particle reactivity

The reactivity of soot alone was studied on the synthetic gas bench. An isothermal oxidation at 570 °C was performed in a simple feed (10% O_2 in N_2). Soot appeared to burn moderately fast at this temperature. The soot oxidation rate vs. conversion is displayed in Fig. 2. Two oxidation stages can be distinguished: a first 'initiation phase' with a rapidly increasing oxidation rate that peaks when soot conversion reaches 10% and a second 'propagation phase' during which oxidation is slower. CO_2 formation is promoted during the initiation phase: the $CO_2/(CO + CO_2)$ ratio peaks at 64% compared to about 56% during the propagation phase (not displayed). These results are in agreement with those obtained by Yezerets et al. [15] which attributed the initial boost in reactivity to the presence of some type of highly reactive surface species like oxygen containing groups. Carbon–oxygen functional groups like C=O, C–O–C or C–OH were actually detected by Müller et al. [16] on diesel soot samples and they are expected to be very reactive sites [9]. The slower oxidation rate observed during the propagation phase is attributed to the oxidation of the remaining C–C bondings of the carbon atoms within the particles.

The comparison of ULSD and B30 soot reactivity on the synthetic gas bench shows that B30 is the most reactive soot during both oxidation phases. This is due to its much larger oxygen content and to its higher BET surface area. This difference in reactivity may be related to the location of the 'C–O' bond inside the soot structure: a 'C–O' bond located at edges would be preferentially oxidized by gaseous O_2, compared to a 'C–C' bond or a 'C–O' bond located inside the basal plane of a graphene layer.

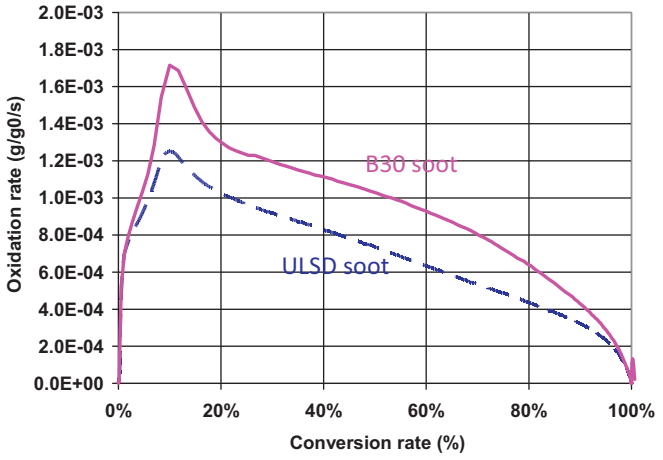

Fig. 2. Soot oxidation rate vs. conversion rate – 570 °C, 10% O_2 in N_2.

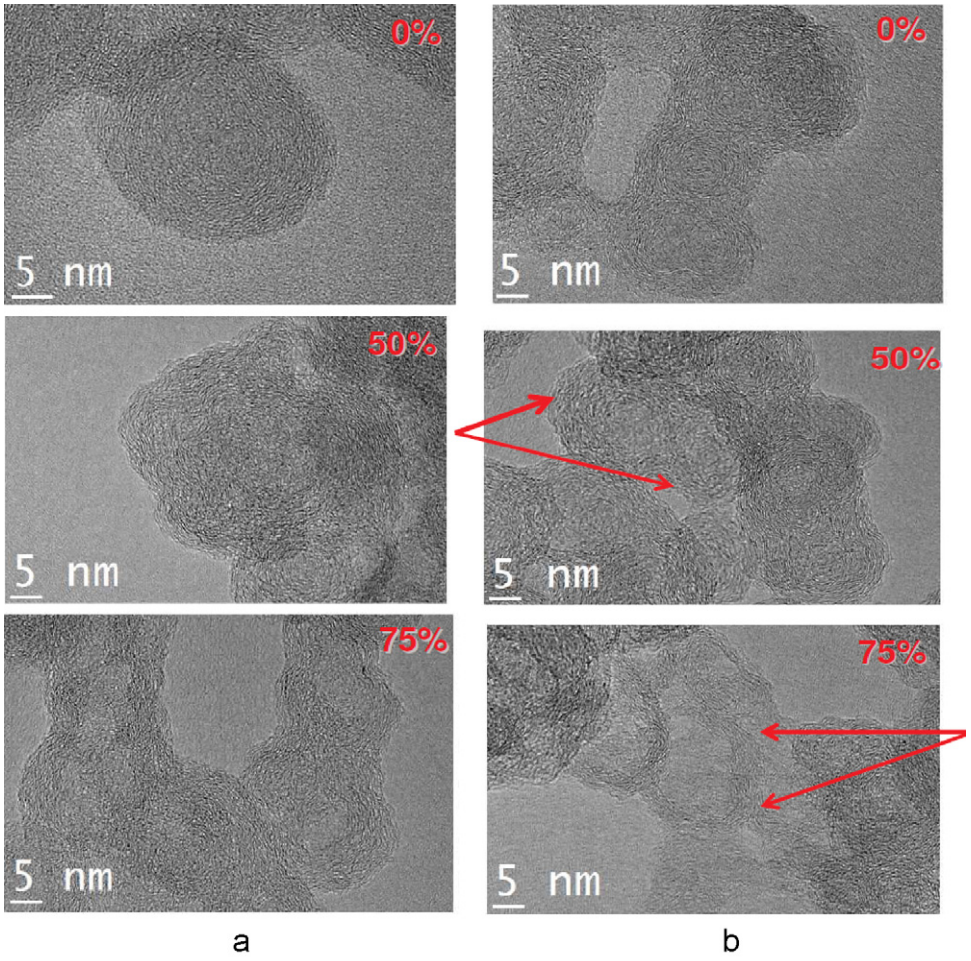

Fig. 3. HRTEM images at 570 °C at three different burnoff stages of ULSD soot (a) and B30 soot (b).

3.4. *Effect of biofuel on particle morphology*

Soot structure was investigated by using high-resolution transmission electron microscopy (HRTEM) in order to find correlations with soot reactivity. HRTEM images are displayed in Fig. 3 for ULSD (Fig. 3(a)) and B30 (Fig. 3(b)) soot samples, before oxidation (top images), and at 50 and 75% conversion. Oxidized soot samples were prepared during isothermal oxidation tests at 570 °C, which were stopped when the desired conversion was reached.

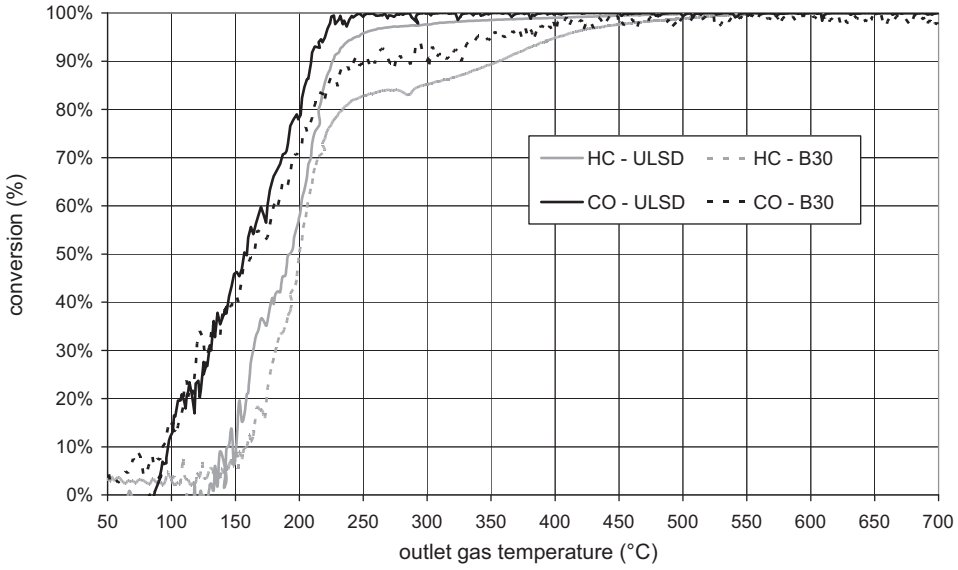

Fig. 4. CO and HC conversion rate measured downstream from the CDPF during a light-off test on ULSD and B30 soot loaded samples – 0.3 equivalence ratio.

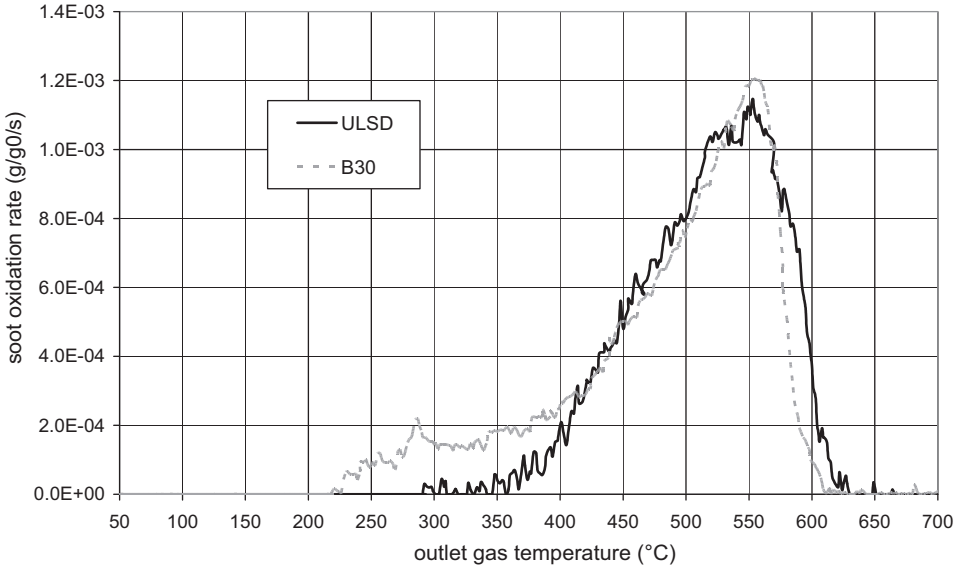

Fig. 5. Soot oxidation rate during a light-off test on ULSD and B30 soot loaded samples – 0.3 equivalence ratio.

HRTEM images of soot in its initial state show a core and shell structure nearly identical between the ULSD and B30 soots: the primary particle appears as an amorphous core surrounded by well-ordered graphene planes. An average particle size of about 23 nm was measured for the two soots on a large set of TEM information, with negligible differences. This shows that the structure and morphology of the collected soot samples are not sufficient to predict differences in soot reactivity. Nevertheless, works from the literature Fig. 4 report that soot structure can evolve in different ways during oxidation, depending on the initial properties of soot.

Compared to its initial state, ULSD soot shows a deterioration of the global organization of carbon planes at 50%. A hollow of about 5 nm in diameter begins to form at 75% conversion, surrounded with short and defective graphene layers. B30 soot exhibits a different oxidation mode. A 5 nm hollow is already visible in primary particles from 50% conversion and pairs of cores combine at 75% conversion into one single hollow surrounded by well-crystallized carbon layers. From 50% conversion, the B30 soot behaviour is in agreement with what was described in the literature for a B100 soot sample: Song et al. [9] found that soot undergoes such an internal burning after 40% burnoff. They suggest that this burning of the more reactive internal carbon occurs once sufficient micropores have been developed to penetrate to the particle core. They attribute the fastest micropore development of the biodiesel type particle to the reaction of the initial oxygen groups leading to short and defective graphene layers.

3.5. Effect of catalytic converter

To further analyze soot reactivity in conditions closer to a realistic engine exhaust line, light-off tests were conducted on soot loaded CDPF samples on the synthetic gas bench. These tests aimed to highlight the interactions that occur on the catalyst between gaseous components and soot in a lean feed typical of a diesel environment (0.3 equivalence ratio).

CO, HC and soot conversion vs. temperature are displayed in Figs. 4 and 5 respectively, for both soot loaded samples. Soot oxidation rate was calculated by subtracting CO_2 emissions due to HC and CO oxidation and CO_2 in the inlet feed from CO_2 measured

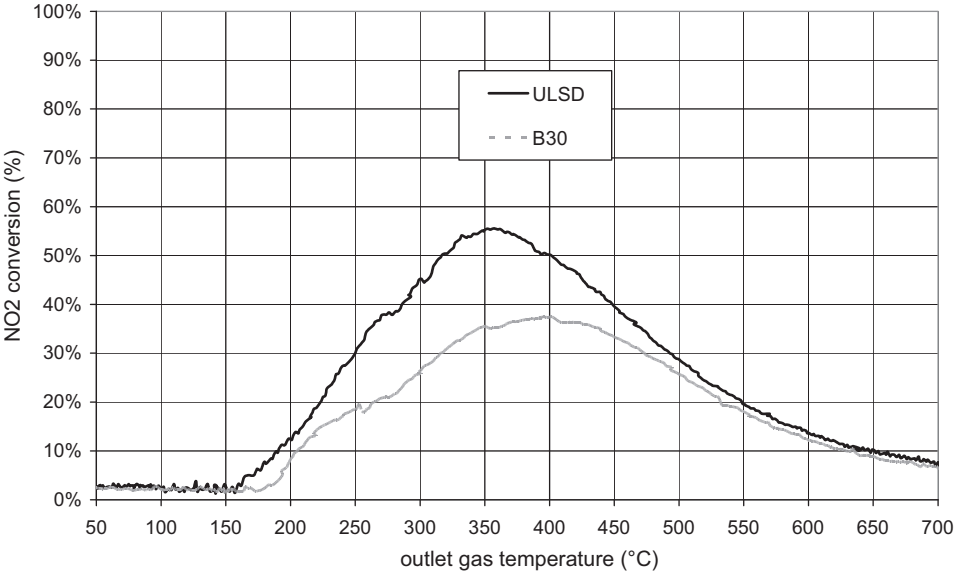

Fig. 6. NO_2 conversion measured downstream from the CDPF during a light-off test on ULSD and B30 soot loaded samples – 0.3 equivalence ratio.

downstream from the catalyst, so as to isolate CO_2 due to soot. This indirect determination appeared to be very repeatable, although the CO_2 analyser had to be used on a large 0–20% range. CO and HC light-off temperatures (50% conversion) are respectively 170 and 200 °C independently of the type of soot. ULSD soot oxidation only becomes significant once a complete HC and CO conversion has been performed, i.e. around 360 °C with a maximum at 550 °C. B30 soot oxidation evolves in a different way. It starts at a lower temperature of 230 °C, with a slow increase until 400 °C where it accelerates to peak at 550 °C. Unlike ULSD soot, the oxidation of B30 soot starts before CO and HC are fully oxidized (conversion is about 85%) and significantly slows down the end of their conversion. NO_2 was measured downstream from the CDPF sample (Fig. 6), as it is known as an efficient oxidising agent of soot at temperatures between 250 °C and 500 °C [12]. The presence of B30 soot appears to have a stronger impact soot on NO_2 emission between 230 and 450 °C, as it decreases by almost 40% compared to ULSD soot. Thermodynamic equilibrium is reached above 450 °C so that soot influence stops at high temperature. Besides its well-known activity as a promoter of CO and HC oxidation, reports suggest that Pt indirectly contributes to soot oxidation by catalysing the oxidation of NO into NO_2 by O_2 [17,18] The impact of soot oxidation on CO and HC conversion can then be ascribed to a competition for Pt catalytic sites, or for oxygen activated and split over from those Pt sites.

4. Conclusions

The behaviour of ULSD and B30 soots in a CDPF was investigated in a synthetic gas bench (SGB) fed with all reactants present in diesel vehicle exhaust gases: CO, HC, NOx, O_2, CO_2, H_2O, etc. B30 soot appears more reactive than ULSD, because of its greater oxygen content and surface area which accelerate its oxidation rate, with internal burning starting from 50% of soot conversion compared to 75% for ULSD soot.

B30 soot starts to oxidize at a lower temperature than ULSD soot due to a stronger impact of NO_2 as an oxidant. This yields significant interactions with CO and HC conversion which are ascribed to a competition to access active Pt sites or for oxygen activated and split over from those Pt sites.

Further tests are needed to complete our global understanding of the reactivity of soot arising from a biodiesel fuel, with the role of the soluble organic fraction. In addition, further soot characterisation by FTIR spectroscopy should allow us to analyze surface oxygen groups, to be correlated to soot reactivity.

Acknowledgements

Support of ADEME for N. Lamharess PhD. grant is gratefully acknowledged. The authors are grateful to S. CASALE for access to the HRTEM facility at UPMC.

References

[1] A.K. Agarwal, Progr. Energy Combust. Sci. 33 (2007) 233–271.
[2] T. Beer, T. Grant, G. Morgan, J. Lapszewicz, P. Anyon, J. Edwards, et al., Comparison of transport fuels. Final report (Ev45a/2/F3c) to the Australian Greenhouse Office on the Stage 2 study of life-cycle emissions analysis of alternative fuels for heavy vehicles, Australia, 2001.
[3] EUCAR /JRC /CONCAWE, Well-to-wheel master presentation, Report WTW_010307 available online: http://ies.jrc.ec.europa.eu/jec-research-collaboration/downloads-jec.html, 2007.
[4] M.S. Graboski, R.L. McCormick, Proc. Energy Combust. Sci. 24 (1998) 125–164.
[5] U.S. Environmental Protection Agency, A comprehensive analysis of biodiesel impacts on exhaust emissions, Draft Technical Report EPA420-P-02-00, National Service Center for Environmental Publications, Cincinnati, OH, 2002.
[6] M.A. Hess, M.J. Haas, T.A. Foglia, Fuel Process. Technol. 88 (2007) 693–699.
[7] A.W. Kandas, I. Gokhan Senel, Y. Levendis, A.F. Sarofim, Carbon 43 (2005) 241–251.
[8] R.L. Van der Wal, A. Yezerets, N.W. Currier, D.H. Kim, C.M. Wang, Carbon 45 (2007) 70–77.
[9] J. Song, M. Alam, A.L. Boehman, U. Kim, Combust. Flame 146 (2006) 589–604.
[10] H. Jung, D.B. Kittelson, M.R. Zachariah, Environ. Sci. Technol. 40 (2006) 4949–4955.
[11] A.M. Peterson, P.I. Lee, M.C. Lai, M.C. Wu, C.L. Di Maggio, S. Ng, H. Tang, J. Eng. Gas Turb. Power-Trans ASME 132 (2010) 11.
[12] C.-N. Millet, R. Chedotal, P. Da Costa, Appl. Catal. B 90 (2009) 339–346.
[13] L. Castoldi, N. Artioli, R. Matarrese, L. Lietti, P. Forzatti, Catal. Today 157 (2010) 384–389.
[14] G. Knothe, Energy Fuels 22 (2008) 1358–1364.
[15] A. Yezerets, N. Currier, H. Eadler, A. Suresh, P. Madden, Catal. Today 88 (2003) 17–25.
[16] J.-O. Müller, D.S. Su, R.E. Jentoft, U. Wild, R. Schlögl, Environ. Sci. Technol. 40 (2006) 1231–1236.
[17] A. Setiabudi, M. Makkee, J.A. Moulijn, Appl Catal. B 42 (2003) 35–45.
[18] L. Castoldi, R. Matarrese, L. Lietti, P. Forzatti, Appl. Catal. B 64 (2006) 25–34.